ON THE USE OF TENSOR PATHS TO ESTIMATE THE NON-PROPORTIONALITY FACTOR OF MULTIAXIAL STRESS OR STRAIN HISTORIES

Marco Antonio Meggiolaro, meggi@puc-rio.br
Jaime Tupiassú Pinho de Castro, jtcastro@puc-rio.br
Department of Mechanical Engineering, Pontifical Catholic University of Rio de Janeiro
Rua Marquês de São Vicente 225 – Gávea, Rio de Janeiro, RJ, 22451-900, Brazil

Hao Wu, wuhao@tongji.edu.cn
Zheng Zhong, zhongk@tongji.edu.cn
School of Aerospace Engineering and Applied Mechanics, Tongji University
Siping Road 1239, 200092, Shanghai, P.R. China

Abstract. *Non-proportional (NP) hardening is an additional strain-hardening effect caused by out-of-phase multiaxial loadings, which activates cross-slip bands in several directions due to the rotation of the maximum shear planes. This hardening increase under NP loads with respect to proportional loadings must be considered in multiaxial fatigue calculations, in special for materials with low stacking fault energy (SFE), such as austenitic stainless steels. NP hardening is not only a function of the material, but depends also on the shape of the load history path in a stress or strain diagram, evaluated through a non-proportionality factor F_{NP} that varies from zero, for a proportional history, to one, for a 90^o out-of-phase tension-torsion loading with same normal and effective shear amplitudes. Originally, F_{NP} was estimated from the aspect ratio of a convex enclosure that contains the load history path, such as an ellipse, but such convex enclosure estimates can lead to poor predictions of F_{NP}. Another approach consists on evaluating the shape of the six-dimensional (6D) path described by the six normal and shear components of the stress tensor, where the stress path contour is interpreted as a homogeneous wire with unit mass. The moment of inertia (MOI) tensor of this hypothetical wire is then calculated and used to estimate F_{NP}. But the use of 6D stress paths to estimate F_{NP} is questionable, since 6D formulations implicitly include the effect of the hydrostatic stress, while NP hardening is caused by the deviatoric plastic straining, not by stresses alone or by their hydrostatic component. In this work, the NP factor F_{NP} of a multiaxial history is estimated from the eigenvalues of the MOI tensor of the plastic strain path, which are associated with the accumulated plastic straining in the principal directions defined by the associated eigenvectors. Experimental results for 14 different multiaxial histories prove the effectiveness of the proposed method.*

Keywords*: multiaxial fatigue, non-proportional loadings, non-proportionality factor, additional hardening, tensor path*

1. INTRODUCTION

Proportional fatigue loads cause isotropic strain-hardening effects that may cyclically harden or soften the tested material. Non-proportional (NP) multiaxial loadings, on the other hand, besides isotropic hardening may cause an additional hardening effect. This phenomenon, called NP hardening, cross-hardening, or additional strain-hardening, depends on the load history, through a non-proportionality factor F_{NP}, and on the material, through an additional hardening constant α_{NP}, where $0 \le \alpha_{NP} \le 1$. Typically, the NP hardening effect is high in austenitic stainless steels at room temperature (e.g. $\alpha_{NP} \cong 1$ for the 316 stainless steel), medium in carbon steels ($\alpha_{NP} \cong 0.3$ for a 1045 steel), and low in aluminum alloys ($\alpha_{NP} \cong 0$ for Al 7075).

NP hardening happens in materials with low stacking fault energy (SFE), which in austenitic stainless steels is only $23mJ/m^2$, and well spaced dislocations, where the slip bands generated by proportional loading are always planar. In these materials, the NP loads activate cross-slip bands in several directions, due to the rotation of the maximum shear planes, increasing the strain-hardening effect with respect to proportional loadings. On the other hand, in materials with close dislocations and high SFE, such as aluminum alloys which typically have SFE values near $250mJ/m^2$, the cross-slip bands already happen naturally even under proportional loading. Hence, NP histories do not cause any significant additional strain-hardening effects in such materials, which have $\alpha_{NP} \cong 0$. Note, however, that α_{NP} depends not only on the material and its microstructure, but also on the strain amplitudes involved in the history (Shamsaei and Fatemi, 2010). In general, lower amplitudes are associated with lower α_{NP}.

When NP hardening is significant, NP load histories can produce fatigue crack initiation lives that are much lower than the ones obtained under proportional histories with the same strain range $\Delta\varepsilon$, since the NP hardening increases the corresponding $\Delta\sigma$ range. Conversely, for materials with large additional hardening α_{NP} under stress-controlled loads, the fatigue lives are much longer under NP loads than under proportional loads with same stress range $\Delta\sigma$, due to the lower strain range $\Delta\varepsilon$ necessary to achieve such $\Delta\sigma$ due to NP hardening.

In general, the NP hardening can be modeled using the same Ramberg-Osgood plastic exponent n' from the cyclic uniaxial σ-ε curve, and using a new coefficient $k_{NP} = k' \cdot (1 + \alpha_{NP} \cdot F_{NP})$, where k' is the uniaxial Ramberg-Osgood plastic

coefficient. Note that NP hardening can multiply the uniaxial cyclic strain hardening coefficient *k'* by a value as high as 2, when both $\alpha_{NP} = 1$ and $F_{NP} = 1$.

To account for NP hardening effects, it is necessary to not only measure α_{NP} but also to correctly evaluate the NP factor F_{NP} associated with the load history. According to Shamsaei and Fatemi (2010), the NP factor depends solely on the shape of the load history path. The largest NP factor, associated with $F_{NP} = 1$, happens for 90° out of phase tension-torsion loading with equal normal and effective shear amplitudes, which generate a circle in the von Mises $\sigma \times \tau\sqrt{3}$ stress or $\varepsilon \times \gamma/\sqrt{3}$ strain diagrams. Note that proportional histories, associated with straight paths that cross the origin of the von Mises stress or strain diagram, do not cause NP hardening.

2. CONVEX ENCLOSURES AND BISHOP'S TENSOR PATH MOMENTS

Originally, F_{NP} was estimated from the aspect ratio of the convex enclosure that contains the load history path, e.g. from the aspect ratio b/a of an enclosing ellipse with semi-axes a and b, called the Minimum F-norm Ellipsoid (Meggiolaro and Castro, 2012). However, such convex enclosure estimates can lead to poor predictions of F_{NP}, as seen in Fig. 1(a). This simple example shows a path that does not encircle the origin of the von Mises $\sigma \times \tau\sqrt{3}$ diagram, while entirely located far away from it. Despite the almost circular shape of the enclosing Minimum F-norm Ellipsoid (MFE), which would suggest $F_{NP} \cong 1$, the principal direction in fact varies very little along such path, since the angle between each point in the path and the origin of the 2D diagram varies very little during each cycle. Therefore, the actual F_{NP} should be very small in this example.

Another simple example of a convex enclosures that fails to calculate F_{NP} is shown in Fig. 1(b), where a loading path describes a straight line that does not cross the origin of the diagram. This particular path induces a 45° variation of the principal direction, implying in $F_{NP} > 0$, however any convex enclosure method would predict $F_{NP} = 0$ for such straight line. The use of the stress path to estimate F_{NP} is also questionable. Figure 1(c) shows a stress path that combines a purely elastic tension-torsion portion (well inside the yield surface with radius S_Y) with uniaxial tension-compression plastic straining. Since NP hardening is caused by plastic straining, the purely elastic portion should not influence the value of F_{NP}. As plastic strains only occur along such path under uniaxial conditions, it is expected that $F_{NP} = 0$, which is confirmed by experiments and by incremental plasticity simulations using Tanaka's NP model (Tanaka, 1994). However, a convex enclosure method applied to such stress path would wrongfully predict F_{NP} much greater than zero, as suggested by the MFE ellipse in Fig. 1(c). Therefore, any accurate F_{NP} estimation method should be based on the plastic strain path, not on the stress or total strain path.

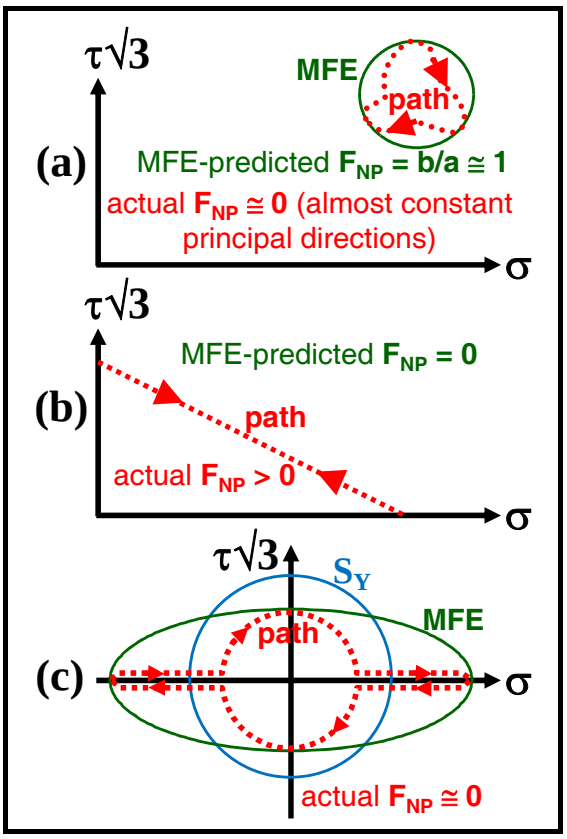

Figure 1. Stress path examples showing the inadequacy of convex enclosure methods, such as the Minimum F-norm Ellipsoid (MFE), to predict mean components or the non-proportionality factor F_{NP}.

To calculate F_{NP} of a general 6D load path, Bishop (2000) introduced a 6 × 6 inertia tensor termed the Rectangular Moment Of Inertia (RMOI) of the stress path, which can be expressed using Voigt-Mandel's vectorial stress representation $\bar{\sigma} \equiv \left[\sigma_x \quad \sigma_y \quad \sigma_z \quad \tau_{xy}\sqrt{2} \quad \tau_{xz}\sqrt{2} \quad \tau_{yz}\sqrt{2} \right]^T$ by

$$I_\sigma \equiv \frac{1}{p_\sigma} \cdot \oint (\bar{\sigma} - \bar{\sigma}_m) \cdot (\bar{\sigma} - \bar{\sigma}_m)^T \cdot |d\bar{\sigma}| \tag{1}$$

where the mean component $\bar{\sigma}_m$ and accumulated stress p_σ are also integrated along the stress path, calculated from

$$\bar{\sigma}_m \equiv \frac{1}{p_\sigma} \cdot \oint \bar{\sigma} \cdot |d\bar{\sigma}| \quad \text{and} \quad p_\sigma \equiv \oint |d\bar{\sigma}| \tag{2}$$

In the above equations, $|d\bar{\sigma}|$ stands for the Euclidean norm of the stress increment $d\bar{\sigma}$, and the superscript T means transpose of a vector. The RMOI stress tensor measures the distribution of the stress path, relative to its mean, about the coordinate planes. Bishop proposed that F_{NP} can be estimated from the two largest eigenvectors $\lambda_{\sigma 1}$ and $\lambda_{\sigma 2}$ of I_σ ($\lambda_{\sigma 1} \geq \lambda_{\sigma 2}$) through

$$F_{NP} = \sqrt{\lambda_{\sigma 2} / \lambda_{\sigma 1}} \tag{3}$$

But NP hardening is caused by plastic straining, which is independent of the hydrostatic stress or strain component. Therefore, the flaws in Bishop's RMOI approach are: (i) it is formulated in a stress space instead of a plastic strain one; (ii) it implicitly assumes that the hydrostatic stress may influence F_{NP}; and (iii) it calculates the RMOI relative to the mean component of the load path, which would wrongfully predict $F_{NP} = 0$ for the path from Fig. 1(b), instead of an $F_{NP} > 0$ that would be obtained from RMOI calculated relative to the origin of the diagram.

To compensate for the flaws in the presented F_{NP} estimates, the Moment Of Inertia (MOI) method, originally proposed by Meggiolaro and Castro (2012) to predict equivalent stress and strain ranges, is extended next to estimate F_{NP} in general 6D NP histories. The MOI method is discussed next.

3. MOMENT OF INERTIA OF PLASTIC STRAIN PATHS

The Moment Of Inertia (MOI) method has been proposed by Meggiolaro and Castro (2012) to calculate alternate and mean components of complex NP load histories. To accomplish that, the history must first be represented in a 5D deviatoric stress or strain space. The MOI method assumes that the load path, represented by a series of points that describe the stress or strain variations along it, is analogous to a homogeneous wire with unit mass. The mean component of the load path is assumed to be located at the perimeter centroid of this hypothetical homogeneous wire shaped as the load history path. The equivalent stress or strain ranges of a loading path are then calculated from the mass moments of inertia (MOI) of the wire, calculated with respect to its perimeter centroid.

In this work, it is proposed that the ideas behind the MOI and Bishop's methods can be applied to calculate the non-proportionality factor F_{NP} of a generic multiaxial load path. Instead of using 5D deviatoric stress or strain spaces, the deviatoric *plastic* strain space E_{5p} is used to represent the load path

$$\bar{e}_p' \equiv [\, e_{1p} \quad e_{2p} \quad e_{3p} \quad e_{4p} \quad e_{5p} \,]^T \tag{4}$$

where the subscript p indicates plastic component and

$$e_{1p} \equiv \varepsilon_{x_p} - \frac{\varepsilon_{y_p} + \varepsilon_{z_p}}{2}, \quad e_{2p} \equiv \frac{\varepsilon_{y_p} - \varepsilon_{z_p}}{2}\sqrt{3}, \quad e_{3p} \equiv \frac{\gamma_{xy_p}}{2}\sqrt{3}, \quad e_{4p} \equiv \frac{\gamma_{xz_p}}{2}\sqrt{3}, \quad e_{5p} \equiv \frac{\gamma_{yz_p}}{2}\sqrt{3} \tag{5}$$

Note that this 5D representation of plastic strains is the same as the one proposed by Tanaka (1994) multiplied by a 1.5 scaling factor, since the identity $\varepsilon_{x_p} + \varepsilon_{y_p} + \varepsilon_{z_p} = 0$ implies that $\varepsilon_{y_p} - \varepsilon_{z_p} = \varepsilon_{x_p} + 2\varepsilon_{y_p}$. There are five motivations to use the proposed 5D projection $\bar{e}_p'$ of the plastic strain space to calculate F_{NP}:

(i) it is a non-redundant representation of the plastic strains, since the linear dependence $\varepsilon_{x_p} + \varepsilon_{y_p} + \varepsilon_{z_p} = 0$ has been removed when projecting the 6D strains onto this 5D sub-space;

(ii) contrary to Bishop's method (Bishop, 2000), the studied path is independent of the hydrostatic components;

(iii) its scaled down version $\bar{e}_p'/1.5$ has been shown by Tanaka (1994) to be appropriate to evaluate the non-proportional hardening evolution in incremental plasticity calculations;
(iv) the Euclidean norm $|\bar{e}_p'|$ is equal to the von Mises equivalent plastic strain, without the need for any scaling factors; and
(v) the direction of such 5D strain vectors is related with the principal direction of the loading.

Thus, to calculate the directions suffering larger plastic strain magnitudes, the plastic strain path in its E_{5p} space can be imagined as a homogeneous wire with unit mass, as it was assumed before for the stress and strain paths in the original MOI method to calculate the equivalent ranges and mean components. This is physically sound, since the moments of inertia of such unit mass wire with respect to the origin are related to how much the path stretches in each considered direction, and therefore they can be correlated with how much accumulated plastic straining there is in such direction. Once the three normal and three shear components of the plastic strain path are obtained, e.g. from incremental plasticity calculations, they must be represented in the five-dimensional E_{5p} space. Figure 2 shows an example of a simple tension-torsion path, whose plastic strains can be represented in the 2D sub-space $e_{1p} \times e_{3p} = 1.5 \cdot (\varepsilon_{xp} \times \gamma_{xyp}/\sqrt{3})$ of E_{5p}.

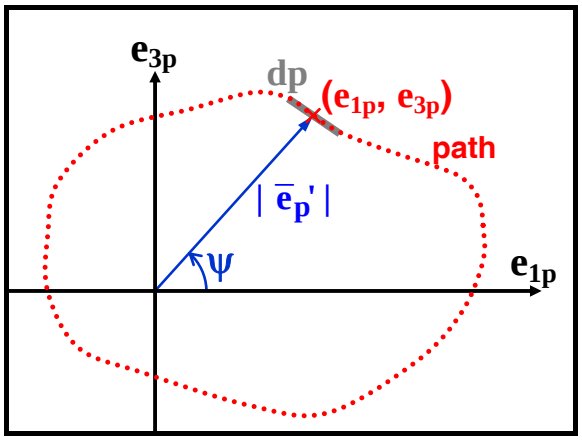

Figure 2. Plastic strain path in the $e_{1p} \times e_{3p} = 1.5 \cdot (\varepsilon_{xp} \times \gamma_{xyp}/\sqrt{3})$ diagram for a tension-torsion history.

Note, however, that the Axial MOI (AMOI) used in the original MOI method, which is the moment of inertia of the path about a given axis, is a measure of how much the path stretches in every *other* direction perpendicular to such axis. In order to calculate how much the path stretches along each individual direction, which can give a measure of its aspect ratio and thus its out-of-phase extent, the Rectangular MOI (RMOI) tensor $\underline{I}_r^O$ of the plastic strain path with respect to the origin O is used instead, which gives the moments of inertia about the planes (or hyperplanes) perpendicular to each considered direction:

$$\underline{I}_r^O = \frac{1}{p} \cdot \oint \bar{e}_p' \cdot \bar{e}_p'^{\,T} \cdot dp \tag{6}$$

where dp is the equivalent plastic strain increment and p is the accumulated plastic strain, defined as

$$dp \equiv \frac{2}{3} \cdot |d\bar{e}_p'| \quad \text{and} \quad p \equiv \oint dp = \frac{2}{3} \cdot \oint |d\bar{e}_p'| = \frac{2}{3} \cdot (\textit{perimeter}) \tag{7}$$

The eigenvalues $\lambda_1, \lambda_2, \ldots, \lambda_5$ ($\lambda_1 \geq \lambda_2 \geq \ldots \geq \lambda_5$) of $\underline{I}_r^O$ are a measure of the accumulated plastic strain along each principal direction defined by the associated eigenvectors. The F_{NP} estimate is here defined as the as the square root of the ratio between the two largest eigenvalues of $\underline{I}_r^O$, i.e.

$$F_{np} = \sqrt{\lambda_2 / \lambda_1} \tag{8}$$

Even though both the MOI and Bishop's methods estimate F_{NP} using similar formulas, their results are quite different, since the former uses the principal RMOI of *deviatoric plastic strain* paths with respect to the *origin O*, while the latter uses the principal RMOI of the *stress* paths with respect to their *mean*.

4. COMPARISONS AMONG F_{NP} PREDICTIONS

The predictions of the NP factor F_{NP} made by using the MOI and the Bishop's methods are now compared to experimental measurements made by Itoh et al. (1995) and by Kida et al. (1997) in a 304 stainless steel with additional hardening coefficient $\alpha_{NP} = 0.9$, Young's modulus $E = 200GPa$, shear modulus $G = 82MPa$, uniaxial cyclic hardening coefficient $k' = 670MPa$ and exponent $n' = 0.125$. Fourteen periodic histories are studied, represented by the strain paths $\varepsilon \times \gamma_{xy}/\sqrt{3}$ shown in Fig. 3 for Cases 0 through 13. The normal strain range $\Delta\varepsilon$ of all studied experimental data is fixed near 0.8%, to avoid issues with the strain amplitude dependence of α_{NP}.

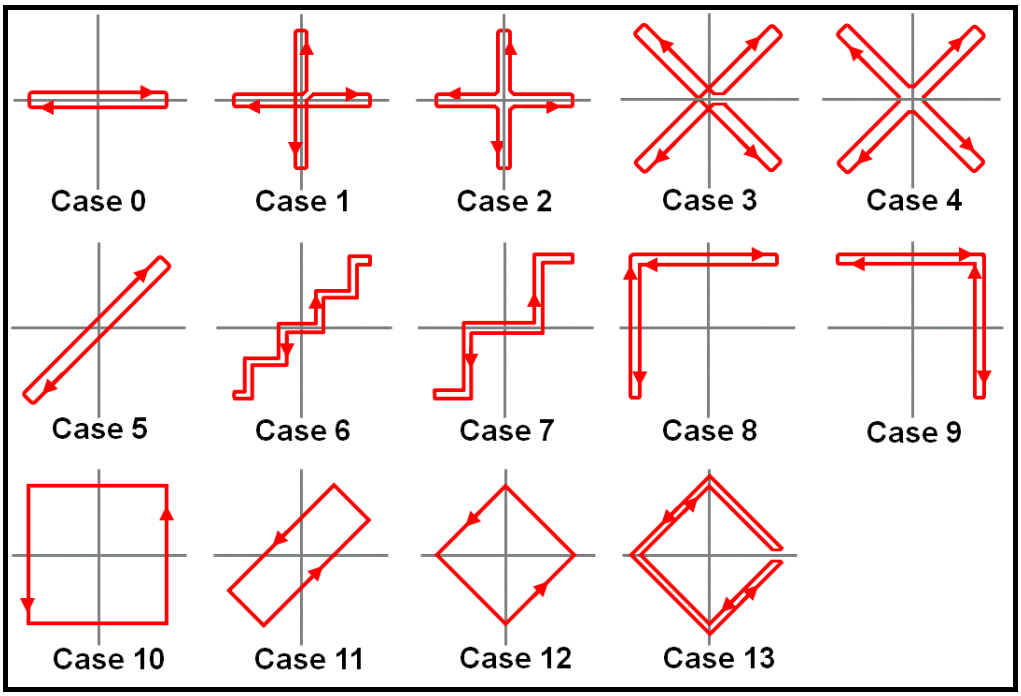

Figure 3. Strain paths $\varepsilon \times \gamma_{xy}/\sqrt{3}$ used in the experimental validation of the F_{NP} predictions.

To evaluate the F_{NP} predictions, an incremental plasticity computer code was specially developed and implemented using the non-linear kinematic model proposed by Jiang and Sehitoglu (1996a), adopting stress increments at each integration step limited to only 2MPa. Jiang's material parameters are calibrated from uniaxial data using the procedure described in (Jiang and Sehitoglu, 1996b), neglecting transient ratcheting effects. For each strain-controlled loading case 0 through 13, the incremental plasticity code is iteratively executed for several candidate values of F_{NP}, until the root mean square (RMS) error between the calculated and the measured strain paths in the $\sigma \times \tau\sqrt{3}$ diagram is minimized. The value of F_{NP} that minimizes the RMS error for each one of the 14 paths is assumed to be the experimental NP factor, which is compared in Fig. 4 with the MOI and Bishop's predictions. As shown in the figure, the MOI method predicts better values for F_{NP} than Bishop's method, which overestimates roughly by a factor of 2 or more the NP factors of load histories with low $0 < F_{NP} < 0.5$ factors such as Cases 6, 7 and 11, for the same reason discussed in the example from Fig. 1(c).

5. CONCLUSIONS

The MOI method is able to predict the non-proportionality factor F_{NP} of multiaxial histories, without the need for adjustable parameters. It predicts the out-of-phase extent of a loading history based on the eigenvalues of the Rectangular Moment Of Inertia of the plastic strain path. This measure of F_{NP} is independent of the particular choice of coordinate system, being invariant under coordinate transformations. Contrary to convex enclosure methods, the MOI method accounts for the contribution of every single segment of the load path, dealing with arbitrarily shaped histories without losing information about their shape. Experimental results demonstrated the effectiveness of the proposed approach for fourteen tension-torsion histories.

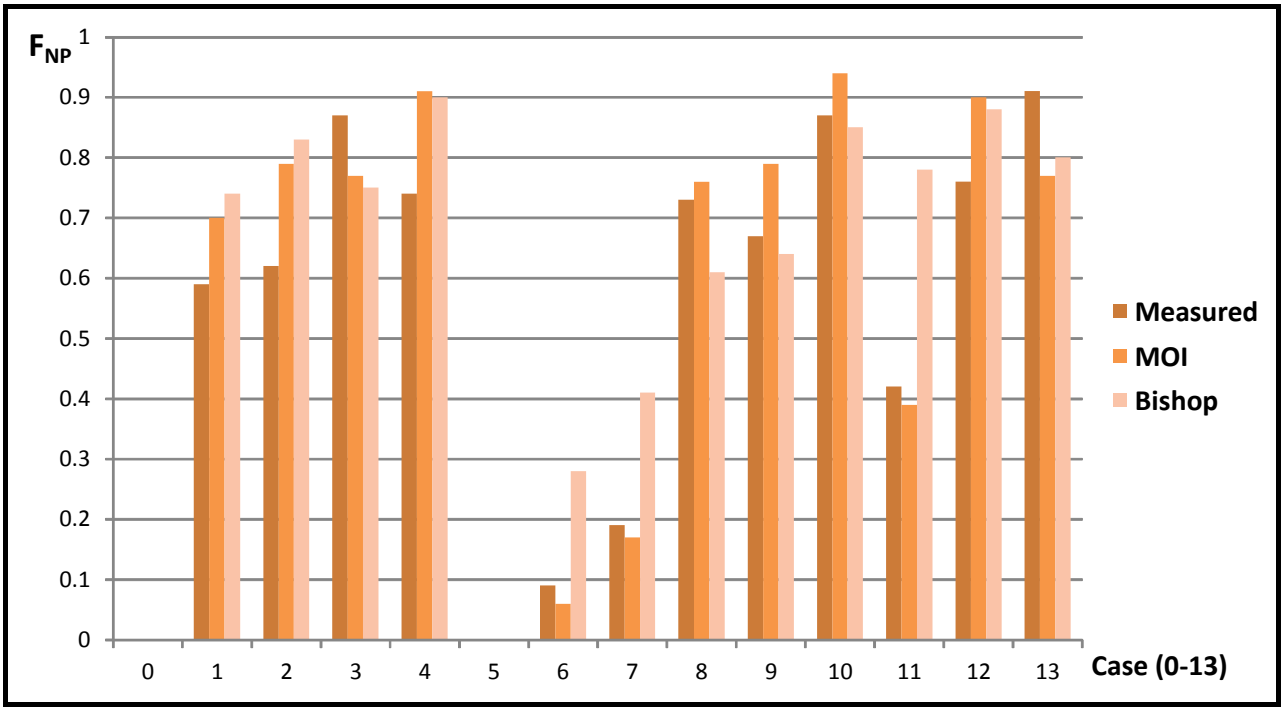

Figure 4. Measured and predicted F_{NP} from the MOI and Bishop's methods for Cases 0 through 13, for a 304 stainless steel at strain range levels near *0.8%*. Note that the proportional Cases 0 and 5 result in zero NP factors.

6. ACKNOWLEDGMENTS

The authors would like to acknowledge Prof. Darrell F. Socie for providing the experimental data used in the analyses. CNPq has provided research scholarships for the authors Marco A. Meggiolaro and Jaime T.P. Castro.

7. REFERENCES

Bishop, J.E., 2000. "Characterizing the non-proportional and out-of-phase extend of tensor paths," Fatigue and Fracture of Engineering Materials and Structures, Vol. 23, pp. 1019-1032.

Itoh, T., Sakane, M., Ohnami, M. and Socie, D.F., 1995. "Nonproportional low cycle fatigue criterion for type 304 stainless steel," ASME Journal of Engineering Materials and Technology, Vol. 117, pp. 285–292.

Jiang, Y. and Sehitoglu, H., 1996a. "Modeling of Cyclic Ratchetting Plasticity, Part I: Development of Constitutive Relations," ASME Journal of Applied Mechanics, Vol. 63, No. 3, pp. 720-725.

Jiang, Y. and Sehitoglu, H., 1996b. "Modeling of Cyclic Ratchetting Plasticity, Part II: Comparison of Model Simulations with Experiments," ASME Journal of Applied Mechanics, Vol. 63, No. 3, pp. 726-733.

Kida, S., Itoh, T., Sakane, M., Ohnami, M. and Socie, D.F., 1997. "Dislocation structure and non-proportional hardening of type 304 stainless steel," Fatigue and Fracture of Engineering Materials and Structures, Vol. 20, pp. 1375-1386.

Meggiolaro, M.A. and Castro, J.T.P., 2012. "An Improved Multiaxial Rainflow Algorithm for Non-Proportional Stress or Strain Histories - Part I: Enclosing Surface Methods," International Journal of Fatigue, Vol. 42, pp. 217-226.

Shamsaei, N. and Fatemi, A., 2010. "Effect of microstructure and hardness on non-proportional cyclic hardening coefficient and predictions," Materials Science and Engineering A 527, pp. 3015–3024.

Tanaka, E., 1994. "A non-proportionality parameter and a cyclic viscoplastic constitutive model taking into account amplitudedependences and memory effects of isotropic hardening," European Journal of Mechanics - A/Solids, Vol. 13, pp. 155–173.

8. RESPONSIBILITY NOTICE

The authors are the only responsible for the printed material included in this paper.